

Controllable Accent Normalization via Discrete Diffusion

Qibing Bai^{1,5}, Yuhan Du⁴, Tom Ko⁶, Shuai Wang^{4,6,**}, Yannan Wang⁵, Haizhou Li^{2,3,6}

¹ SDS, ² SAI, and ³ SRIBD, The Chinese University of Hong Kong, Shenzhen, China

⁴ School of Intelligence Science and Technology, Nanjing University, Suzhou, China

⁵ Tencent Ethereal Audio Lab, Tencent, Shenzhen, China

⁶ Shenzhen Loop Area Institute, Shenzhen, China

qibingbai@link.cuhk.edu.cn, shuaiwang@nju.edu.cn

Abstract

Existing accent normalization methods do not typically offer control over accent strength, yet many applications—such as language learning and dubbing—require tunable accent retention. We propose DLM-AN, a controllable accent normalization system built on masked discrete diffusion over self-supervised speech tokens. A Common Token Predictor identifies source tokens that likely encode native pronunciation; these tokens are selectively reused to initialize the reverse diffusion process. This provides a simple yet effective mechanism for controlling accent strength: reusing more tokens preserves more of the original accent. DLM-AN further incorporates a flow-matching Duration Ratio Predictor that automatically adjusts the total duration to better match the native rhythm. Experiments on multi-accent English data show that DLM-AN achieves the lowest word error rate among all compared systems while delivering competitive accent reduction and smooth, interpretable accent strength control¹.

Index Terms: accent conversion, diffusion language model, speech synthesis, voice conversion, controllability

1. Introduction

Accent conversion (AC) seeks to alter speech from one accent to another while preserving the speaker’s characteristics. A special case, accent normalization (AN)², converts non-native (L2) accented speech into a native (L1) accented form. AN technology enables a wide range of applications, including pronunciation training for language learners [1], authentic dubbing in multimedia [2], and personalized text-to-speech systems [3].

Early deep learning approaches for AN are *reference-based* [4–7], relying on native accent speech samples to generate accent-neutral representations via PPG features [4, 5, 7] or native TTS [6]. *Reference-free methods* [8–10] eliminate this requirement by directly mapping between accented and native representations, though they still rely on parallel data. Subsequent work removes the parallel data constraint through ASR–TTS pipelines [11], accent feature disentanglement [12], or TTS-guided representations [13, 14], further augmented with flow matching [15] and normalizing flow [16]. However, these approaches depend on TTS-synthesized targets, whose quality can be limited by voice cloning and duration modeling errors.

Recent token-based methods [17–20] offer a promising alternative. TokAN [19] quantizes speech into self-supervised discrete tokens, performs autoregressive token-to-token conversion, and recovers waveforms via a flow-matching synthe-

sizer. CosyAccent [21] adopts a non-autoregressive direct flow-matching approach and introduces a “source-synthesis” data strategy. Both systems support total-duration control. However, none of the above methods provides control over accent strength—a desirable capability for gradual accent reduction or accent preservation as part of speaker identity. The only attempt at accent strength control [22] manipulates the starting timestep of a continuous diffusion process, but it operates under a frame-to-frame framework with fixed duration, lacking fine-grained rhythm adjustability and duration control.

In this paper, we propose DLM-AN, a controllable accent normalization system based on masked discrete diffusion over self-supervised speech tokens. DLM-AN extends the LLaDA diffusion language model [23] to speech: a bidirectional Transformer iteratively predicts masked tokens conditioned on content representations from a CTC-guided [24] token encoder. The key insight enabling controllability is that, under a phonetically rich tokenizer, native and accented renditions of the same utterance share many tokens in similarly pronounced regions but differ in accent-affected regions. We introduce a Common Token Predictor (CTP) that identifies tokens likely shared with the native target. By reusing high-confidence source tokens to initialize the masked sequence, users can smoothly control accent strength—from full normalization (all tokens generated from scratch) to near-resynthesis (all source tokens preserved). A flow-matching Duration Ratio Predictor further provides explicit control over the total output duration.

Our contributions are as follows:

- We propose the first accent normalization system based on discrete diffusion, enabling iterative token generation conditioned on phonemically guided content representations.
- We introduce a common token predictor that provides smooth, interpretable accent strength control through threshold-based source token reuse.
- We demonstrate that DLM-AN achieves the best content preservation (lowest WER) among all compared systems, while offering competitive naturalness and accent reduction, along with robust duration scaling.

2. Related Work

2.1. Controllability in Accent Conversion

Most accent conversion/normalization systems perform a one-shot “full” accent shift without a user-controllable knob [5, 20]. Recently, controllability has attracted increasing attention, motivated by applications such as gradual accent reduction in language learning and adjustable accent retention in dubbing.

One line of work studies duration control (speech-rate control) during accent normalization. TokAN [19] performs token-

**indicates the corresponding author.

¹Samples: <https://P1ping.github.io/dlman-demo/>

²Also referred to as foreign accent conversion (FAC).

to-token conversion with self-supervised discrete units and supports duration preservation. CosyAccent [21] further enables explicit duration scaling via a duration-ratio predictor and proposes a source-synthesis data strategy to reduce reliance on TTS-synthesized supervision artifacts.

In contrast, controllable *accent strength* (i.e., smoothly trading off normalization vs. retaining the original L2 accent) remains less explored. FAC-FACodec [22] introduces an intensity control mechanism in a diffusion-based, factorized-codec framework by using the diffusion starting timestep as a user knob. Related directions include fine-grained controllable accent transfer models [25], controllable accented TTS that renders accent intensity at coarse/fine levels [26], and scalable accented TTS with automated accent label discovery [27].

Our work leverages masked discrete diffusion over speech tokens to support both total-duration control and an interpretable accent-strength knob via source-token reuse; the iterative masking/unmasking procedure also naturally supports localized correction (speech infilling).

2.2. Self-Supervised Speech Tokens

Discrete tokens derived from self-supervised learning (SSL) representations [28, 29] correlate strongly with phonetic content [30], which makes them attractive units for speech generation and conversion. Such tokens have been adopted in token-based voice conversion [31–33] and high-fidelity speech generation/TTS frameworks [34]. More broadly, discreteness allows importing “text-like” modeling techniques into speech, including spoken language modeling [35], direct speech-to-speech translation [36], and speech-centric LLM systems [37].

Recent work also explores SSL tokens for ASR, including multilingual ASR [38], contextual ASR with Zipformer [39], and accent-robust discrete-token ASR modeling [40]. For accent conversion/normalization, discrete tokens have been studied under different supervision regimes, including zero-shot/minimally-supervised conversion [18], pseudo-parallel mapping [17, 19], and prompt-based imitation [20]. We leverage WavLM [29] to extract discrete tokens for conversion and synthesis, capitalizing on its strong phonetic encoding and noise robustness.

2.3. Discrete Diffusion

Discrete diffusion has recently been investigated for text generation (i.e., diffusion language models), adapting continuous diffusion principles to categorical data like tokens. Two commonly used formulations are: (i) multinomial/categorical diffusion, where tokens transition probabilistically across the vocabulary [41, 42], and (ii) masked/absorbing diffusion, where tokens are progressively mapped to a special absorbing state (e.g., $[\text{MASK}]$) and then iteratively recovered [23, 42].

For the absorbing diffusion process, consider a sequence of discrete tokens $\mathbf{x}_0 \in \{1, \dots, V\}^n$, where V is the vocabulary size and n is the sequence length. The forward process adds noise independently per token over T timesteps:

$$q(\mathbf{x}_t | \mathbf{x}_{t-1}) = \prod_{i=1}^n \left[(1 - \beta_t) \delta_{x_t^i = x_{t-1}^i} + \beta_t \delta_{x_t^i = [\text{MASK}]} \right] \quad (1)$$

where $\beta_t \in (0, 1)$ is the time-dependent masking probability, and $[\text{MASK}]$ is an additional absorbing state ($V + 1$). The cumulative forward process is:

$$q(\mathbf{x}_t | \mathbf{x}_0) = \text{Cat}(\mathbf{x}_t; \bar{\alpha}_t \mathbf{x}_0 + (1 - \bar{\alpha}_t) \mathbf{e}_{[\text{MASK}]}) \quad (2)$$

with $\bar{\alpha}_t = \prod_{s=1}^t (1 - \beta_s)$ and $\mathbf{e}_{[\text{MASK}]}$ the one-hot vector for the mask token. At $t = T$, \mathbf{x}_T is fully masked with high probability.

The reverse process is parameterized by a neural network $p_\theta(\mathbf{x}_{t-1} | \mathbf{x}_t)$, typically a Transformer predicting a categorical distribution over tokens.

Masked diffusion is widely adopted for diffusion language models (e.g., LLaDA [23]), where the forward process randomly masks tokens at varying ratios, and the reverse process predicts masked positions in parallel using a bidirectional Transformer. This provides a principled variational lower bound on likelihood, contrasting autoregressive models. Compared with masked generation (e.g., MaskGIT [43], MaskGCT [44], Metis [45]), masked diffusion has a better theoretical foundation, as it optimizes an evidence lower bound (ELBO) and supports iterative refinement.

The log-likelihood admits the evidence lower bound (ELBO):

$$\log p(\mathbf{x}_0) \geq \mathbb{E}_{q(\mathbf{x}_{1:T} | \mathbf{x}_0)} \left[\log \frac{p_\theta(\mathbf{x}_{0:T})}{q(\mathbf{x}_{1:T} | \mathbf{x}_0)} \right] \quad (3)$$

Maximizing the ELBO is equivalent to minimizing the following loss, which decomposes into a reconstruction term at $t=0$ and KL divergences for $t > 0$:

$$\begin{aligned} \mathcal{L}(\theta) = & \mathbb{E}[-\log p_\theta(\mathbf{x}_0 | \mathbf{x}_1)] \\ & + \sum_{t=2}^T D_{\text{KL}}(q(\mathbf{x}_{t-1} | \mathbf{x}_t, \mathbf{x}_0) \| p_\theta(\mathbf{x}_{t-1} | \mathbf{x}_t)) \\ & + D_{\text{KL}}(q(\mathbf{x}_T | \mathbf{x}_0) \| p(\mathbf{x}_T)) \end{aligned} \quad (4)$$

In practice, a simplified loss is used, often reweighted cross-entropy on predicting the original tokens from noisy inputs. For instance, LLaDA derives a continuous-time upper bound on the negative log-likelihood. For $t \sim \mathcal{U}[0, 1]$, the loss is

$$\mathcal{L}(\theta) = -\mathbb{E}_{t, \mathbf{x}_0, \mathbf{x}_t} \left[\frac{1}{t} \sum_{i: x_t^i = [\text{MASK}]} \log p_\theta(x_0^i | \mathbf{x}_t) \right] \quad (5)$$

where the expectation is approximated via Monte Carlo sampling over uniform t (masking rate), data \mathbf{x}_0 , and corrupted \mathbf{x}_t . The $1/t$ reweighting arises from the continuous-time ELBO derivation, ensuring each masking rate contributes proportionally to the bound.

Surveys on discrete diffusion highlight its growing role in LLMs [46]. Notable directions include SEDD [47], which extends score matching to discrete spaces through score entropy, and ReMDM [48], which enables iterative refinement via re-masking of previously generated tokens. Entropy-bounded unmasking [49] further accelerates sampling from masked diffusion models. More recently, corrective diffusion language models [50–53] explicitly supervise visible incorrect tokens, enabling discriminative confidence and targeted correction in parallel decoding scenarios.

3. Methodology

We propose to use a diffusion language model (DLM) for controllable accent normalization. The method is shortened “DLM-AN”. Figure 1 shows the pipeline of DLM-AN. The SSL tokenizer extracts SSL representations from the L2-accented waveform and quantize the features into discrete tokens. A Transformer token encoder takes further processes these tokens, producing continuous content representations. To make the content representations phonemic enough, a CTC-based phonemic

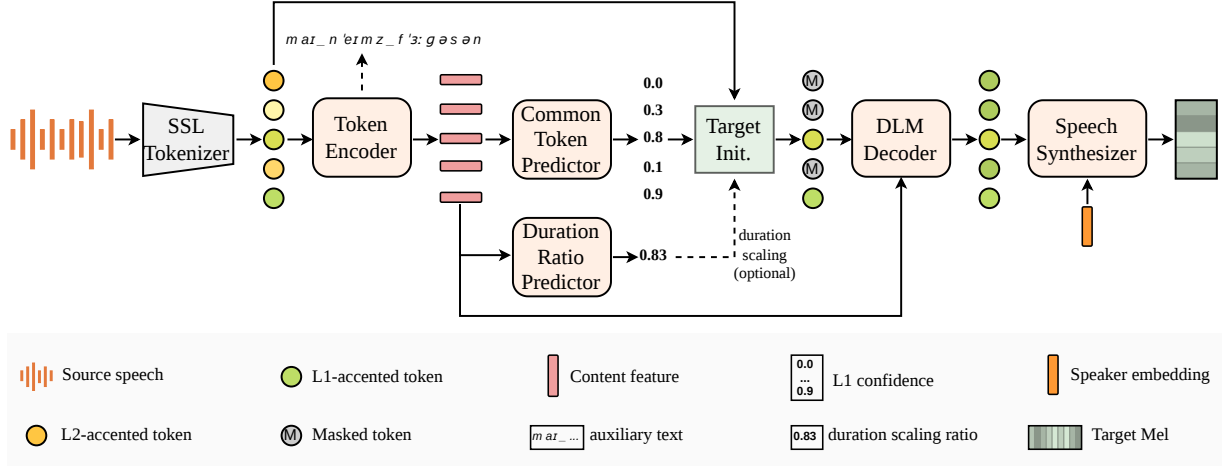


Figure 1: Overview of the DLM-AN pipeline. The SSL tokenizer extracts discrete tokens from L2-accented speech. A Transformer token encoder with CTC-based phonemic guidance produces content representations, which are fed into the Common Token Predictor (CTP), Duration Ratio Predictor (DP), and the DLM decoder. The DLM decoder iteratively generates the target token sequence, optionally initialized with high-CTP-confidence source tokens. A flow-matching synthesizer and vocoder produce the final waveform.

guidance is imposed upon them, shown as the auxiliary text in Figure 1. The content representations are further taken as the input for three modules: Common Token Predictor (CTP), Duration Ratio Predictor (DP), and the DLM decoder.

Note that the content features are concatenated with the source tokens (embeddings) when feeding to CTP and DP, in order to provide detailed pronunciation patterns (i.e., phonetic information). This concatenation is not displayed in Figure 1 for brevity.

CTP predicts whether each token is common in both the source and target sequences. The higher the score for a token, the more probable this token is associated with a native pronunciation, as will be demonstrated in the subsequent sections. Tokens with high CTP scores could be optionally “reused” for the decoding/generation process later. DP predicts the ratio of the total duration: $\text{dur}_{\text{tgt}}/\text{dur}_{\text{src}}$. This ratio can be optionally used to determine the total duration/length of the target sequence.

Given the target duration ratio, either predicted, arbitrarily specified, or kept 1.0 to maintain the source duration, the length of the initial target sequence is determined. By default, the initial target sequence is purely filled with [MASK] for generation from scratch. Optionally, based on the CTP scores and a given threshold or proportion, certain source tokens can be reused to initialize the target sequence. After the initial target sequence is determined, the DLM decoder iteratively generates the entire target sequence, conditioned on the content features from the token encoder.

The more tokens reused in the target sequence, the more source accent is expected to be preserved. The speech synthesizer further generates the corresponding Mel-spectrogram given the target tokens, conditioned on the speaker embedding extracted from the input source speech. The Mel-spectrogram can be converted to a waveform using the HiFT vocoder [54].

3.1. Discrete Diffusion for Speech Tokens

We extend the LLaDA masked diffusion language model [23] to discrete speech tokens for controllable accent normalization. Our forward corruption process uses pure absorbing masking, parameterized by a timestep $t \sim \mathcal{U}[0, 1]$ per sequence.

Let $\mathbf{y}_0 \in \{1, \dots, V\}^L$ be a clean speech token sequence, where V is the speech vocabulary size and L is the sequence

length. We define the absorbing masking rate as $\lambda = (1 - \epsilon)t + \epsilon$, with $\epsilon > 0$. Each position i is masked independently:

$$q_\lambda(z_i | y_0^i) = \lambda \delta_{z_i = [\text{MASK}]} + (1 - \lambda) \delta_{z_i = y_0^i} \quad (6)$$

which induces a masked index set M and a visible set $\bar{M} = [L] \setminus M$. The corrupted sequence \mathbf{z} has corruption set $\mathcal{C} = M$. The model $p_\theta(\mathbf{y}_0 | \mathbf{z}, \mathbf{c})$ is a bidirectional Transformer that predicts the original tokens from \mathbf{z} , conditioned on the content representations \mathbf{c} from the token encoder. The training objective follows LLaDA:

$$\mathcal{L}(\theta) = -\mathbb{E}_{t, \mathbf{y}_0, \mathbf{z}} \left[\frac{1}{\lambda} \sum_{i \in M} \log p_\theta(y_0^i | \mathbf{z}, \mathbf{c}) \right] \quad (7)$$

approximated by Monte Carlo sampling with global per-token normalization for stability. This objective optimizes a principled upper bound on the negative log-likelihood, enabling strong bidirectional reasoning and iterative refinement.

The DLM decoder has a decoder-only Transformer structure without causal masking, allowing parallel prediction over masked positions. The content representations \mathbf{c} are integrated as conditional inputs via self-attention to guide accent-normalized generation while preserving content.

During inference, we employ a greedy sampling algorithm with optional initialization: start from a fully or partially masked sequence (reusing high-CPT-confidence tokens), and iteratively predict and unmask positions based on confidence scores, conditioned on \mathbf{c} . For enhanced quality, we use classifier-free guidance (CFG) [55]: compute both conditional logits $p_\theta(\mathbf{y}_0 | \mathbf{z}, \mathbf{c})$ and unconditional logits $p_\theta(\mathbf{y}_0 | \mathbf{z}, \emptyset)$, then combine them as $p_{\text{cfg}} = (1 + w_{\text{DLM}})p_\theta(\cdot | \mathbf{z}, \mathbf{c}) - w_{\text{DLM}}p_\theta(\cdot | \mathbf{z}, \emptyset)$, where w_{DLM} is the guidance strength. This amplifies the conditioning signal for better content preservation.

The structure of DLM decoder is shown in Figure 2. It features a self-attention-only structure (i.e., using self-attention to fuse the conditional information). The input is basically two sequences: the content features and the noised target tokens. Three special tokens, [START], [TASK], and [END], are added to wrap and separate the two sequences, guiding the DLM behavior.

To make the condition reusable across time steps (i.e., token sequences with different numbers of masked tokens), the

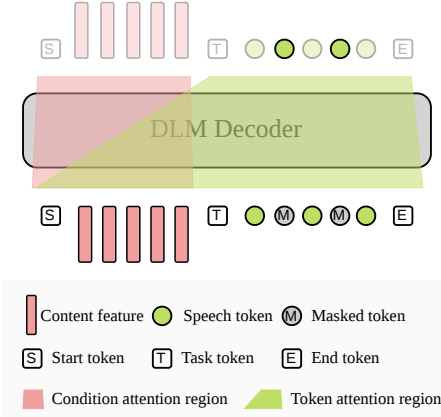


Figure 2: Structure of the DLM decoder. The input consists of the content features and the noised target tokens, separated by special tokens [START], [TASK], and [END]. The content features are mutually attentive but do not attend to the token sequence (pink region), while the token sequence attends to the entire input (green region).

content features are mutually attentive but with no attention to the token sequence. In contrast, the token sequence can attend to the entire input sequence. The attention regions of the two parts are depicted in Figure 2 with the colors pink and green, respectively.

3.2. Common Token Prediction

With a sufficiently phonetic tokenizer, utterances spoken with different accents tend to share many tokens in similarly pronounced regions, while differing mainly in accent-affected regions. Motivated by this property, we introduce a Common Token Predictor (CTP) that assigns each source token a confidence score indicating how likely it is to be shared with the (native) target. Tokens with high CTP confidence can be reused to initialize the target sequence, providing a simple and interpretable control of accent strength: reusing more tokens preserves more of the source accent. We formulate CTP as a sequence-tagging

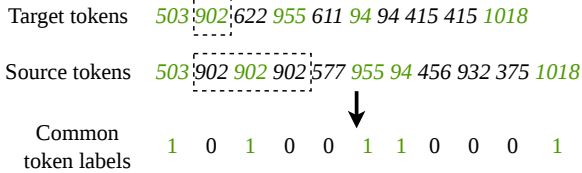


Figure 3: Extraction of common token labels via the longest common subsequence (LCS) between source and target token sequences. For consecutive identical tokens with differing durations, center-mode alignment is applied (dashed rectangle).

problem. Given paired source and target token sequences, we derive binary labels by computing the longest common subsequence (LCS) between them. LCS has been used previously to evaluate accent conversion models [18]; here we use it to identify which source tokens are shared with the target. The label extraction procedure is illustrated in Figure 3. We obtain the LCS via dynamic programming and backtracking. For consecutive identical tokens that have different durations in the source and target, we apply a center alignment: only the centered tokens are marked positive (dashed rectangle in Figure 3).

The training objective for CTP is binary cross-entropy loss. Let S be the source sequence length, and let $\mathbf{l} \in \{0, 1\}^S$ be the

binary labels derived from the LCS searching. Given the source content features, the CTP module (parameterized by ϕ) outputs predicted probabilities $\hat{\mathbf{l}} \in [0, 1]^S$. The loss is:

$$\mathcal{L}_{\text{CTP}}(\phi) = -\frac{1}{S} \sum_{i=1}^S [l_i \log \hat{l}_i + (1 - l_i) \log(1 - \hat{l}_i)]. \quad (8)$$

3.3. Duration Ratio Prediction

Because L2-accented speech often exhibits different rhythm and speaking rate, directly inheriting the source total duration can lead to sub-optimal naturalness. DLM-AN therefore includes a duration ratio predictor (DP) that estimates the global duration ratio $r = \text{dur}_{\text{tgt}}/\text{dur}_{\text{src}}$. DP uses a diffusion Transformer (DiT) [56] backbone with an attentive pooling layer, and is trained with conditional flow matching.

The training objective for DP is conditional flow matching loss [57]. Let $r > 0$ be the target duration ratio (ground truth $\text{dur}_{\text{tgt}}/\text{dur}_{\text{src}}$), and let \mathbf{c} be the input content representations from the token encoder. The flow matching model $v_\psi(u_t, t, \mathbf{c})$ (parameterized by ψ) predicts the velocity field:

$$u_t = (1 - t)u_0 + tr, \quad (9)$$

where $t \sim \mathcal{U}[0, 1]$ and $u_0 \sim \mathcal{N}(0, 1)$ is a standard normal prior. The loss is:

$$\mathcal{L}_{\text{DP}}(\psi) = \mathbb{E}_{t, u_0} [\|v_\psi(u_t, t, \mathbf{c}) - (r - u_0)\|^2] \quad (10)$$

This objective trains the model to generate duration ratios conditioned on \mathbf{c} , enabling global rhythm adjustment. In practice, we also condition DP on the source token embeddings to capture fine-grained pronunciation details; we omit this from the formulation for brevity.

3.4. Phoneme Guidance and Joint Training

The token encoder is a Transformer with relative positional embeddings, producing content representations \mathbf{c} . The CTP and DP modules also use Transformer backbones with relative positional embeddings. The DLM decoder is a self-attention-only Transformer with two-block masking, using rotary positional encoding (RoPE) [58] for the entire sequence.

To encourage \mathbf{c} to be phonemically informative, we impose a CTC-based phonemic guidance on the token encoder outputs. Concretely, we attach a linear projection head on top of the token encoder to predict phoneme logits, and compute a CTC loss against phoneme label sequences derived from the corresponding transcripts. Given phoneme sequence \mathbf{p} , the loss is

$$\mathcal{L}_{\text{CTC}} = \text{CTC}(\text{Linear}(\mathbf{c}), \mathbf{p}) \quad (11)$$

We train the token-prediction modules jointly, including the token encoder, CTP, DP, and DLM decoder, following a two-stage schedule of pretraining and fine-tuning as described in the experimental setup. Let \mathcal{L}_{DLM} denote the masked discrete diffusion loss for token generation (Eq. (7)). The overall joint-training objective is:

$$\mathcal{L}_{\text{token}} = \mathcal{L}_{\text{DLM}} + \beta_1 \mathcal{L}_{\text{DP}} + \beta_2 \mathcal{L}_{\text{CTP}} + \beta_3 \mathcal{L}_{\text{CTC}} \quad (12)$$

The token-prediction modules are pre-trained on native-only data and fine-tuned on semi-synthesized parallel data.

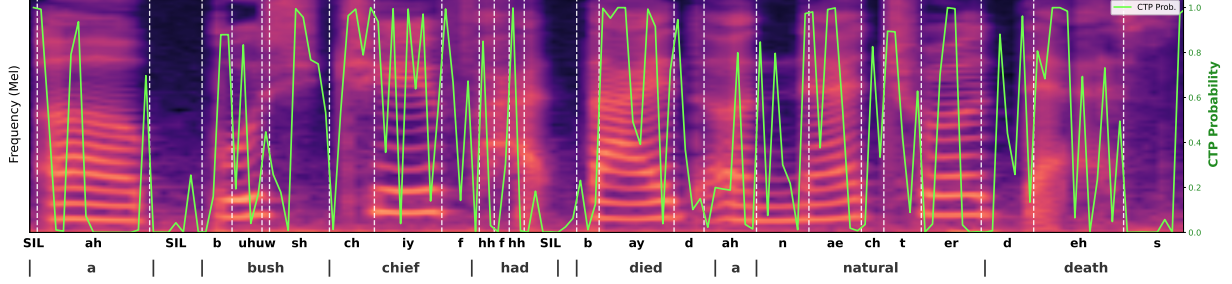


Figure 4: Visualization of common token prediction for a Chinese-accented sample. CTP confidence values are overlaid on the Mel-spectrogram. PPG-predicted phonemes are shown below and their boundaries (white dashed lines) are overlaid on the spectrogram. Aligned words are shown at the bottom. Regions with prominent L2 accent (e.g., prolonged “a”, unclear “had”, /S/-like ending of “death”) receive low CTP confidence.

3.5. Sampling Algorithm for Token Conversion

After processing the source L2-accented tokens with the token encoder, CTP, and DP, we can then initialize the target token sequence and use the DLM decoder to complete it (i.e., “Target Init.” and “DLM Decoder” in Figure 1). By default, we use the greedy sampler with a threshold-based strategy for reusing source tokens, as demonstrated in Sec. 5.1.2 and Algorithm 1.

Algorithm 1 Greedy sampling with CTP-based initialization.

Require: Source tokens \mathbf{y}^{src} (length N_{src}) and duration ratio r
CTP scores $\{l_i\}_{i=1}^{N_{\text{src}}}$, reuse threshold τ , sampling steps T
Content representations \mathbf{c} and CFG strength w_{DLM}

Ensure: Target tokens \mathbf{y}^{tgt}

- 1: $N_{\text{tgt}} \leftarrow \text{round}(N_{\text{src}} \cdot r)$
- 2: $K \leftarrow \lceil N_{\text{tgt}}/T \rceil$ ▷ tokens to unmask per step
- 3: $\mathcal{I} \leftarrow \{i \mid l_i > \tau\}$ ▷ reused source-token indices
- 4: Initialize $\mathbf{z}^{(0)}$ by nearest interpolation from source to target
length: $\mathbf{z}^{(0)} \in \{1, \dots, V, [\text{MASK}]\}^{N_{\text{tgt}}}$
- 5: **for** $j = 1$ to N_{tgt} **do**
- 6: $i^* \leftarrow \text{round}\left(\left(j - \frac{1}{2}\right) \frac{N_{\text{src}}}{N_{\text{tgt}}} + \frac{1}{2}\right)$ ▷ source index
- 7: **if** $i^* \in \mathcal{I}$ **then**
- 8: $z_j^{(0)} \leftarrow y_{i^*}^{\text{src}}$
- 9: **else**
- 10: $z_j^{(0)} \leftarrow [\text{MASK}]$
- 11: **end if**
- 12: **end for**
- 13: $N_{\text{mask}} \leftarrow |\{j \mid z_j^{(0)} = [\text{MASK}]\}|$
- 14: $T_{\text{eff}} \leftarrow \lceil N_{\text{mask}}/K \rceil$, $s_0 \leftarrow \max(1, T - T_{\text{eff}} + 1)$ ▷ start step from reuse proportion
- 15: **for** $s = s_0$ to T **do**
- 16: Compute logits at masked positions:
 $\ell_{\text{cond}}(\cdot \mid \mathbf{z}^{(s-1)}, \mathbf{c})$ and $\ell_{\text{uncond}}(\cdot \mid \mathbf{z}^{(s-1)})$
- 17: Apply CFG: $\ell_{\text{cfg}} \leftarrow (1 + w_{\text{DLM}}) \ell_{\text{cond}} - w_{\text{DLM}} \ell_{\text{uncond}}$
- 18: For each masked position j , set $\hat{y}_j \leftarrow \arg \max \ell_{\text{cfg}}(j)$
and confidence $\gamma_j \leftarrow \max \text{softmax}(\ell_{\text{cfg}}(j))$
- 19: Select \mathcal{J} as the top-min(K , $|\text{masked}|$) masked positions by γ_j
- 20: Unmask: set $z_j^{(s)} \leftarrow \hat{y}_j$ for $j \in \mathcal{J}$; keep all other positions unchanged
- 21: **end for**
- 22: **return** $\mathbf{y}^{\text{tgt}} \leftarrow \mathbf{z}^{(T)}$

3.6. Token-to-Speech Synthesis

We use a flow-matching speech synthesizer with a vocoder [54] to generate waveforms. The input token sequence is encoded by a relative-positional Transformer encoder, and the encoded features are concatenated with a speaker embedding before being fed into a DiT decoder. The speech synthesizer is trained separately on native-only speech data. Similar to CosyAccent, DLM-AN deploys a two-way CFG strategy for generation:

$$\begin{aligned} \bar{v}_\eta(\mathbf{x}_t, t, \mathbf{y}, \mathbf{s}) &= v_\eta(\mathbf{x}_t, t, \mathbf{y}, \mathbf{s}) \\ &+ w_1(v_\eta(\mathbf{x}_t, t, \mathbf{y}, \mathbf{s}) - v_\eta(\mathbf{x}_t, t, \emptyset, \mathbf{s})) \\ &+ w_2(v_\eta(\mathbf{x}_t, t, \mathbf{y}, \mathbf{s}) - v_\eta(\mathbf{x}_t, t, \mathbf{y}, \emptyset)) \end{aligned} \quad (13)$$

where v_η is the synthesizer, $t \in [0, 1]$ is the time variable, \mathbf{x}_t is the Mel-spectrogram at time t , \mathbf{y} is the input tokens, and \mathbf{s} is the speaker embedding. The two CFG factors w_1 and w_2 control the emphasis on the content and timbre conditions, respectively.

4. Experimental Setup

4.1. Datasets

The experiments are conducted on English. Training uses the English subset of Emilia [59] (Emilia-EN) and the LibriTTS-R corpus [60] with synthesized L2-accented counterparts³ [21]. We also use the L2-ARCTIC corpus [61] together with four American speakers from ARCTIC [62]. We further synthesize pseudo native targets for this extended L2-ARCTIC set, which are used for supervised fine-tuning and evaluation. The pseudo native targets are generated using a native-only zero-shot Matcha-TTS [63] model trained on LibriTTS-R.

Emilia-EN is solely used for pretraining. LibriTTS-R is used to train the SSL tokenizer and the flow-matching speech synthesizer. For fine-tuning, both augmented LibriTTS-R (with synthesized source utterances) and extended L2-ARCTIC (with synthesized targets) are utilized.

Since the L2-accented counterparts [21] of LibriTTS-R were synthesized using prompts drawn from L2-ARCTIC, we adopt the same train-valid-test partition of L2-ARCTIC to prevent text leakage.

4.2. Tokenizer

The proposed method relies on the phonetic richness of the speech tokens. We use WavLM_{large} and extract layer-22 representations for tokenization. We train an online K-Means model with 1024 clusters (codebook size 1024) on LibriTTS-R.

³<https://huggingface.co/datasets/Piping/L2-LibriTTSR/>

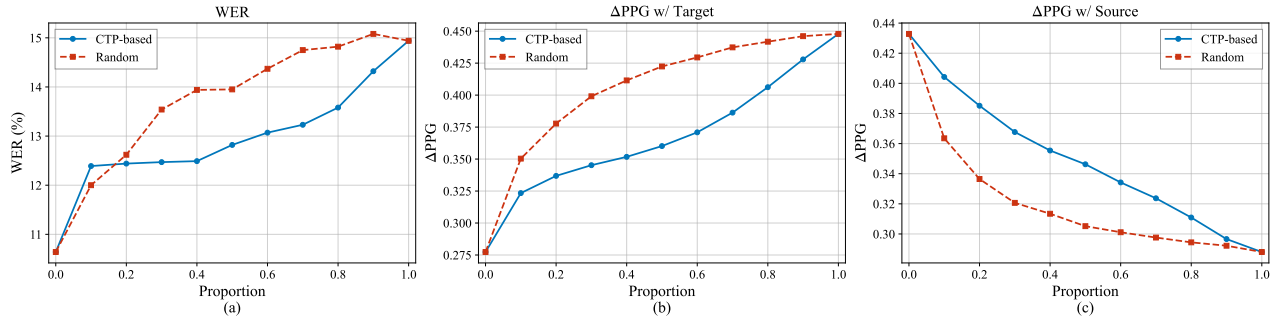


Figure 5: CTP-based vs. random token selection at varying reuse proportions. Three metrics are compared: (a) WER, (b) ΔPPG with the L1-accented target, and (c) ΔPPG with the L2-accented source. CTP-based selection achieves generally lower WER and consistently better accent separation than random selection at the same proportion.

4.3. Compared Systems

We evaluate our model against two strong baselines:

- *TokAN* [19]: An autoregressive model operating on deduplicated tokens. It recovers token-wise durations in the speech synthesis stage. This model features a flow matching duration predictor with two conditions: 1) the token sequence and 2) the average token duration. When provided with the average token duration, TokAN is able to preserve the total duration. We test two modes: *TokAN-1*, which predicts token durations directly, and *TokAN-2*, which predicts with total-duration awareness and preserves the total duration.
- *CosyAccent* [21]: A non-autoregressive direct flow-matching model. It features a total-duration ratio predictor similar to our proposed model. It can be regarded as a continuous-diffusion counterpart of the proposed model, but without accent-strength control. We test two modes: *CosyAccent-1*, which predicts the total duration ratio, and *CosyAccent-2*, which inherits the source total duration.

For the token-reuse setting of DLM-AN, we deploy a threshold-based selection strategy: tokens with CTP confidence higher than a threshold (τ) are reused. For simplicity, we do not apply token reuse and duration scaling simultaneously. We evaluate four configurations of DLM-AN:

- *DLM-AN-1*: Uses the predicted total duration ratio.
- *DLM-AN-2* ($\tau = 1.0$): Inherits the source total duration while predicting the target sequence from scratch.
- *DLM-AN-2* ($\tau = 0.3$): Inherits the source total duration, with a threshold for common token prediction (i.e., $\tau = 0.3$).
- *DLM-AN-2* ($\tau = 0.0$): Inherits all the source tokens (i.e., direct resynthesis).

For TokAN and DLM-AN, the two token-based systems, we pretrain them on Emilia-EN. BART-style [18, 64] token corruption is applied to the source token sequence. This helps avoid teaching the model to trivially copy the source sequence. Different from the original TokAN, no source accent embedding is utilized. Given the corrupted source sequence, TokAN performs autoregressive generation while DLM-AN performs masked generation. TokAN and DLM-AN share a similar architecture: a speech token encoder with CTC-based phonemic guidance, a self-attention-only decoder, and a flow-matching speech synthesizer. TokAN predicts token-wise durations in the synthesizer module, whereas DLM-AN predicts the total duration ratio during token-level conversion. For DLM-AN, we set the loss weights in Eq. (12) as $\beta_1=1.0$, $\beta_2=1.0$, and $\beta_3=0.2$ for joint training of the token-prediction modules. For CTP training, we use a positive weight of 2 for better label balance.

For TokAN generation, we use beam search with a beam size of 10. For DLM-AN, we use the greedy sampler with 32 steps; the CFG guidance strength w_{DLM} is set to 1.0. For the speech synthesizers in TokAN and DLM-AN, we use the Euler sampler with 32 steps. The CFG strengths w_1 and w_2 are set to 1.0 and 1.0, respectively.

For CosyAccent, we use the official `Whispermedium` model [65] as the frozen speech frontend. CosyAccent is also pre-trained on Emilia-EN, with the encoder supervised only by the CTC loss. During inference, we use the same CFG weights and number of sampling steps as in the original paper.

Resemblyzer⁴ is deployed to extract speaker embeddings for the speech synthesizer modules in all the compared models. The final waveform is generated using the HiFTNet vocoder [54] from CosyVoice2 [66].

4.4. Evaluation Data & Metrics

Evaluation Set. Our test set involves the extended L2-ARCTIC dataset, as described in Sec. 4.1. The test set covers seven accents: Arabic, Chinese, Hindi, Korean, Spanish, Vietnamese, and native American English. The set contains 80 sentences. The partitioning is consistent with the source-synthesis training data [21], with no text leakage in the training data.

Subjective Evaluation. We conducted listening tests with 25 raters to assess three qualities: *Naturalness (NAT)* and *Accentedness (ACT)* were measured via MUSHRA tests. The native accent was excluded from the ACT evaluation. *Speaker Similarity (SIM)* was measured via Best-Worst Scaling (BWS), with scores aggregated using a standard counting algorithm [67]: $(N_{best} - N_{worst}) / N_{occurrence}$.

Objective Evaluation. We use four objective metrics to assess conversion quality automatically. *Intelligibility*: Word Error Rate (WER) from a native-only ASR model⁵ to simulate listener perception. *Naturalness*: The UTMOSv2 score⁶ from a neural naturalness predictor. *Timbre Preservation*: Speaker Encoding Cosine Similarity (SECS) using the accent-robust Resemblyzer. *Accentedness Reduction*: The phonetic posteriorgram distance (ΔPPG)⁷ [68]. By default, ΔPPG is computed between generated utterances and the synthesized native targets, but some analyses also compute it against the source to measure how much accent is removed.

⁴<https://github.com/resemble-ai/Resemblyzer>

⁵<https://huggingface.co/facebook/s2t-medium-librispeech-asr>

⁶<https://github.com/sarulab-speech/UTMOSv2>

⁷<https://github.com/interactiveaudiolab/ppgs>

Table 1: Evaluation results of accent normalization systems. Source-length indicates whether the source total duration is preserved. τ denotes the CTP threshold for token reuse ($\tau=1.0$: generation from scratch; $\tau=0.0$: full token reuse / resynthesis). Best and second-best objective results are in **bold** and underlined.

System	Source-length	Subjective			Objective			
		NAT (\uparrow)	ACT (\downarrow)	SIM (\uparrow)	WER (% \downarrow)	UTMOS (\uparrow)	SECS (\uparrow)	Δ PPG (\downarrow)
Source	\checkmark	58.36 \pm 2.84	48.46 \pm 2.61	-	15.86	2.80 \pm 0.41	-	0.5097
TokAN-1 [19]	\times	63.85 \pm 2.49	<u>23.58</u> \pm 1.85	-0.082	13.82	3.07 \pm 0.36	0.8495	0.2884
TokAN-2 [19]	\checkmark	59.20 \pm 2.60	28.01 \pm 2.21	-0.051	14.00	2.97 \pm 0.38	0.8530	0.2980
CosyAccent-1 [21]	\times	61.12 \pm 2.42	25.75 \pm 1.89	-0.071	12.40	2.99 \pm 0.34	0.8294	0.2736
CosyAccent-2 [21]	\checkmark	56.35 \pm 2.61	29.51 \pm 2.12	0.051	13.84	2.89 \pm 0.36	0.8358	0.3029
DLM-AN-1	\times	<u>62.20</u> \pm 2.46	22.94 \pm 1.85	-0.133	<u>11.19</u>	<u>3.05</u> \pm 0.34	0.8385	0.2811
DLM-AN-2 ($\tau=1.0$)	\checkmark	59.50 \pm 2.61	27.90 \pm 2.16	-0.020	10.64	2.93 \pm 0.37	0.8521	<u>0.2773</u>
DLM-AN-2 ($\tau=0.3$)	\checkmark	57.35 \pm 2.59	31.34 \pm 2.34	<u>0.098</u>	12.52	2.90 \pm 0.39	<u>0.8590</u>	<u>0.3580</u>
DLM-AN-2 ($\tau=0.0$)	\checkmark	56.41 \pm 2.70	38.37 \pm 2.57	0.208	14.94	2.86 \pm 0.39	0.8646	0.4479

5. Results

5.1. Effectiveness of Common Token Prediction

For effective common token prediction, higher confidence should be assigned to native-accented regions, whereas low confidence scores should be assigned to highly-L2-accented regions. Figure 4 is a visualization of common token prediction for a Chinese-accented sample. The common token confidence values are displayed over the spectrogram. Phonemes predicted by ppgs [68] are displayed below the spectrogram, with their boundaries being the white dashed lines on the Mel-spectrogram. Aligned words, obtained via MFA [69], are displayed at the bottom. Accent can be determined from the comparison between the words and phonemes. Some prominent L2-accented patterns can be found: 1) the initial word ‘‘a’’ is heavily lengthened; correspondingly, the CTP confidence becomes low in the prolonged part. 2) The PPG-predicted phonemes for the word ‘‘had’’ is messy, corresponding with general low confidence scores. 3) The ending phoneme of ‘‘death’’ is detected as highly similar to /S/, receiving low confidence scores.

5.1.1. Proportion-based Reuse

To progressively preserve or remove the source accent, we can directly control the proportion of reused source tokens based on the CTP confidence scores. However, random reuse may also yield a coarse accent-retention effect. To verify the benefit of CTP-based reuse, we vary the reuse proportion under two strategies—CTP-based selection and random selection. Figure 5 reports three metrics: 1) WER, 2) Δ PPG to the L1-accented target, and 3) Δ PPG to the L2-accented source. Ideally, WER should increase as the reuse proportion increases. In contrast, Δ PPG to the target should decrease (more native-like), while Δ PPG to the source should increase (less similar to the accented input).

Both strategies follow these general trends, but their outcomes differ. CTP-based selection generally yields lower WER than random selection at the same reuse proportion. Moreover, it consistently achieves higher Δ PPG to the source and lower Δ PPG to the target, indicating better accent removal while remaining closer to the native reference. This suggests that CTP indeed prioritizes more native-accented regions for reuse, whereas random selection more frequently preserves highly accented tokens. Overall, CTP-based token reuse provides a more reliable control knob for progressive accent normalization.

5.1.2. Threshold-based Reuse

Input utterances exhibit different strengths of L2 accent. Therefore, enforcing the same reuse proportion for all sources can be suboptimal. We instead adopt threshold-based reuse, where tokens are reused if their CTP confidence exceeds a threshold τ (Algorithm 1). This makes the effective reuse proportion adaptive to the input accent strength.

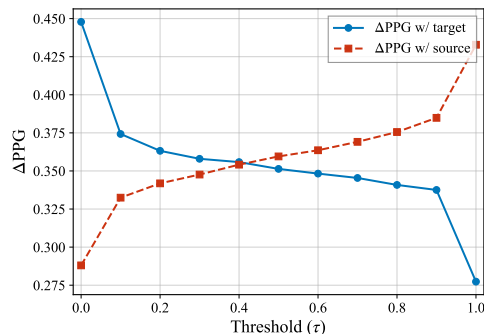


Figure 6: Δ PPG with the L2-accented source and L1-accented target at varying CTP thresholds τ . Lower τ retains more source tokens. As τ increases, Δ PPG with the source increases (more accent removed) while Δ PPG with the target decreases (closer to native).

Figure 6 shows Δ PPG to the source and to the L1-accented target under different thresholds. When $\tau=0.0$, all tokens are reused; as τ increases, fewer tokens are kept; and when $\tau=1.0$, generation from scratch is performed. As expected, Δ PPG to the source increases monotonically with τ , while Δ PPG to the target decreases, confirming that τ provides an interpretable and effective knob for accent reduction.

5.2. Comparison with Baselines

5.2.1. Duration-free Conversion

The main results are shown in Table 1. We first compare the systems under the *free duration* setting (‘‘-1’’ variants), where the model predicts its own target duration. DLM-AN-1 achieves the lowest ACT score (22.94) among all systems, indicating the strongest accent reduction, while attaining the second-highest NAT score (62.20), close to TokAN-1 (63.85) and above CosyAccent-1 (61.12). In terms of objective content preservation, DLM-AN-1 obtains a WER of 11.19%, notably

lower than TokAN-1 (13.82%) and CosyAccent-1 (12.40%). The UTMOS score (3.05) is also competitive with TokAN-1 (3.07), both outperforming CosyAccent-1 (2.99). These results suggest that DLM-AN achieves the best overall balance of accent reduction and content preservation under free duration.

5.2.2. Source-duration-preserved Conversion

Under the *source-duration-preserved* setting (“-2” variants), DLM-AN-2 ($\tau=1.0$) again achieves the best WER (10.64%) and a competitive Δ PPG (0.2773) among all systems. As expected, preserving the source duration generally leads to higher ACT scores and lower NAT scores compared with free-duration counterparts across all models, as the L2-accented rhythm is retained. Notably, DLM-AN-2 ($\tau=1.0$) attains a similar Δ PPG with DLM-AN-1 (0.2773 vs. 0.2811) yet a higher ACT (27.90 vs. 22.94). This suggests that Δ PPG primarily captures segmental (more phonetic) similarity, whereas human raters perceive accentedness more holistically—rhythm and prosody, which are largely determined by duration, play a substantial role in subjective accent judgments.

5.2.3. Controllable Accent Normalization

The effect of the CTP-based token reuse is clearly visible across the DLM-AN-2 variants. As the threshold τ decreases from 1.0 to 0.0, more source tokens are preserved, leading to a progressive increase in ACT (27.90 \rightarrow 31.34 \rightarrow 38.37), reflecting stronger retention of the source accent. Correspondingly, the SIM score rises monotonically ($-0.020 \rightarrow 0.098 \rightarrow 0.208$), confirming that preserving more source tokens improves perceived speaker similarity. The SECS scores follow the same trend (0.8521 \rightarrow 0.8590 \rightarrow 0.8646), with the full-reuse variant achieving the highest timbre preservation. This correlation between the source accent and speaker identity aligns with the finding in [22].

Meanwhile, WER degrades mildly (10.64 \rightarrow 12.52 \rightarrow 14.94) and Δ PPG increases (0.2773 \rightarrow 0.3580 \rightarrow 0.4479), as reusing accented tokens inevitably retains some non-native pronunciation patterns. At $\tau=0.0$ (complete resynthesis), the output closely mirrors the source accent, as indicated by the ACT score (38.37) approaching the source (48.46), demonstrating smooth and interpretable accent strength control.

5.3. Arbitrary Duration Scaling

All three systems support total-duration specification, but via different mechanisms: TokAN predicts token-wise durations after accent normalization, CosyAccent directly generates a target-length spectrogram, and DLM-AN generates a target-length token sequence. To compare robustness under different target lengths, we vary the total-duration ratio and compare WER across systems.

Figure 7 shows the results. DLM-AN achieves the lowest WER (i.e., best content preservation) when the source duration is preserved, and its advantage is more pronounced when the specified ratio is smaller than 1.0. When the target duration is set to half of the source, TokAN degrades substantially because the generated token sequence (after deduplication) is often longer than the desired duration, forcing tokens to be discarded in the synthesis stage. DLM-AN maintains an advantage until the ratio reaches 1.5, likely because such extreme stretching is rare in the training data.

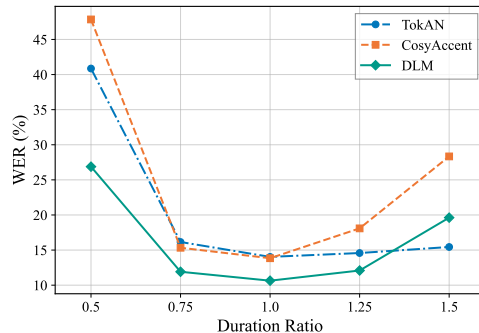


Figure 7: WER (%) at varying duration scaling ratios for TokAN, CosyAccent, and DLM-AN. DLM-AN achieves the lowest WER across most ratios, with a notable advantage under compression (ratio < 1.0).

5.4. Ablation Study

The ablation results are shown in Table 2, which is based on DLM-AN-2 that generates target tokens from scratch. We ablate two factors: 1) CFG in token generation, 2) pretraining on Emilia-EN. The results show the effectiveness of these training/inference components in the proposed DLM-AN.

Table 2: Ablation results of DLM-AN-2 ($\tau=1.0$).

System	WER (% \downarrow)	SECS (\uparrow)	Δ PPG (\downarrow)
Source	15.86	-	0.5097
DLM-AN	10.64	0.8521	0.2773
w/o CFG	11.23	0.8488	0.2907
w/o pretraining	16.61	0.8513	0.3306

6. Conclusion & Future Work

We presented DLM-AN, a controllable accent normalization system based on masked discrete diffusion over self-supervised speech tokens. By introducing a Common Token Predictor (CTP) that identifies source tokens likely shared with the native target, DLM-AN provides a simple yet effective accent-strength knob: reusing more high-confidence tokens preserves more of the original accent, while generating all tokens from scratch yields full normalization. A duration ratio predictor further enables total-duration adjustment. Experiments on multi-accent English data show that DLM-AN achieves the lowest WER among all compared systems, competitive naturalness and accent reduction, and smooth, interpretable accent strength control across a continuous range.

Several directions remain for future work. First, the current pipeline relies on a recognition-based token encoder for phoneme supervision, whose errors can propagate and degrade conversion quality for heavily accented inputs. Second, repeated pronunciations can arise during unmasking; incorporating corrective mechanisms [50, 53] may mitigate such artifacts. Third, the SSL tokenizer and synthesizer are trained on native-only data, potentially limiting reconstruction of highly accented speech; incorporating L2-accented data could improve robustness. Forth, replacing the K-Means tokenizer with learned discrete codebooks (e.g., vector quantization [70]) may yield better phonetic discriminability and further enhance controllability.

7. Generative AI Use Disclosure

Generative AI tools were used solely for editing and polishing the manuscript text. No part of the scientific content, including the ideas, methodology, experiments, or analysis, was generated by AI. All authors have reviewed and take full responsibility for the content of this paper.

8. References

- [1] D. Felps, H. Bortfeld, and R. Gutierrez-Osuna, "Foreign accent conversion in computer assisted pronunciation training," *Speech communication*, vol. 51, no. 10, pp. 920–932, 2009.
- [2] O. Türk and L. M. Arslan, "Subband based voice conversion," in *Proc. Interspeech*, 2002, pp. 289–292.
- [3] L. Sun, H. Wang, S. Kang, K. Li, and H. M. Meng, "Personalized, cross-lingual tts using phonetic posteriorgrams," in *Proc. Interspeech*, 2016, pp. 322–326.
- [4] Z. Guanlong, S. Sinem, L. John, C.-H. Evgeny, and G.-O. Ricardo, "Accent conversion using phonetic posteriorgrams," in *Proc. ICASSP*, 2018, pp. 5314–5318.
- [5] G. Zhao, S. Ding, and R. Gutierrez-Osuna, "Foreign accent conversion by synthesizing speech from phonetic posteriorgrams," in *Proc. Interspeech*, 2019, pp. 2843–2847.
- [6] W. Li, B. Tang, X. Yin, Y. Zhao, W. Li, K. Wang, H. Huang, Y. Wang, and Z. Ma, "Improving accent conversion with reference encoder and end-to-end text-to-speech," *arXiv preprint arXiv:2005.09271*, 2020.
- [7] S. Ding, G. Zhao, and R. Gutierrez-Osuna, "Accentron: Foreign accent conversion to arbitrary non-native speakers using zero-shot learning," *Computer Speech & Language*, vol. 72, p. 101302, 2022.
- [8] G. Zhao, S. Ding, and R. Gutierrez-Osuna, "Converting foreign accent speech without a reference," *TASLP*, vol. 29, pp. 2367–2381, 2021.
- [9] T.-N. Nguyen, N.-Q. Pham, and A. Waibel, "Accent conversion using pre-trained model and synthesized data from voice conversion," in *Proc. Interspeech*, 2022, pp. 2583–2587.
- [10] W. Quamer, A. Das, J. Levis, E. Chukharev-Hudilainen, and R. Gutierrez-Osuna, "Zero-shot foreign accent conversion without a native reference," in *Proc. Interspeech*, 2022, pp. 4920–4924.
- [11] S. Liu, D. Wang, Y. Cao, L. Sun, X. Wu, S. Kang, Z. Wu, X. Liu, D. Su, D. Yu *et al.*, "End-to-end accent conversion without using native utterances," in *Proc. ICASSP*, 2020, pp. 6289–6293.
- [12] M. Jin, P. Serai, J. Wu, A. Tjandra, V. Manohar, and Q. He, "Voice-preserving zero-shot multiple accent conversion," in *Proc. ICASSP*, 2023.
- [13] Y. Zhou, Z. Wu, M. Zhang, X. Tian, and H. Li, "Tts-guided training for accent conversion without parallel data," *Signal Processing Letters*, vol. 30, pp. 533–537, 2023.
- [14] X. Chen, J. Pei, L. Xue, and M. Zhang, "Transfer the linguistic representations from tts to accent conversion with non-parallel data," in *Proc. ICASSP*, 2024.
- [15] Q. Bai, S. Wang, Z. Liu, M. Zhang, W. Rao, Y. Wang, and H. Li, "Diffusion-based method with tts guidance for foreign accent conversion," in *Proc. ISCSLP*, 2024, pp. 284–288.
- [16] T. N. Nguyen, S. Akti, N. Q. Pham, and A. Waibel, "Improving pronunciation and accent conversion through knowledge distillation and synthetic ground-truth from native tts," in *ICASSP*, 2025.
- [17] T.-N. Nguyen, Q. Pham, and A. Waibel, "Accent conversion using discrete units with parallel data synthesized from controllable accented tts," in *Synthetic Data's Transformative Role in Foundational Speech Models*, 2024, pp. 51–55.
- [18] Z. Jia, H. Xue, X. Peng, and Y. Lu, "Convert and speak: Zero-shot accent conversion with minimum supervision," in *Multimedia*, 2024.
- [19] Q. Bai, S. Inoue, S. Wang, Z. Jiang, Y. Wang, and H. Li, "Accent normalization using self-supervised discrete tokens with non-parallel data," in *Interspeech 2025*, 2025, pp. 1618–1622.
- [20] X. Zhang, X. Zhang, K. Peng, Z. Tang, V. Manohar, Y. Liu, J. Hwang, D. Li, Y. Wang, J. Chan, Y. Huang, Z. Wu, and M. Ma, "Vevo: Controllable zero-shot voice imitation with self-supervised disentanglement," in *ICLR*, 2025.
- [21] Q. Bai, S. Shi, S. Wang, Y. Ju, Y. Wang, and H. Li, "Cosyaccent: Duration-controllable accent normalization using source-synthesis training data," *Proc. ICASSP 2026*, 2026.
- [22] Y. Halychanskyi, C. Churchwell, Y. Wen, and V. Kindratenko, "Fac-facodec: Controllable zero-shot foreign accent conversion with factorized speech codec," *Proc. ICASSP 2026*, 2026.
- [23] S. Nie, F. Zhu, Z. You, X. Zhang, J. Ou, J. Hu, J. Zhou, Y. Lin, J.-R. Wen, and C. Li, "Large language diffusion models," *arXiv preprint arXiv:2502.09992*, 2025.
- [24] A. Graves, S. Fernández, F. Gomez, and J. Schmidhuber, "Connectionist temporal classification: labelling unsegmented sequence data with recurrent neural networks," in *ICML*, 2006.
- [25] L. Wang, Z. Yu, Y. Yang, S. Gao, C. Mao, and Y. Huang, "Non-parallel accent transfer based on fine-grained controllable accent modelling," in *EMNLP 2023*. Association for Computational Linguistics, 2023, pp. 9288–9298.
- [26] R. Liu, B. Sisman, G. Gao, and H. Li, "Controllable accented text-to-speech synthesis with fine and coarse-grained intensity rendering," *IEEE/ACM Transactions on Audio, Speech, and Language Processing*, vol. 32, p. 2188–2201, Apr. 2024.
- [27] H. L. Xinyuan, Z. Cai, A. Garg, K. Duh, L. P. García-Perera, S. Khudanpur, N. Andrews, and M. Wiesner, "Scalable controllable accented tts," in *Proc. ASRU 2025*, 2025.
- [28] W.-N. Hsu, B. Bolte, Y.-H. H. Tsai, K. Lakhotia, R. Salakhutdinov, and A. Mohamed, "Hubert: Self-supervised speech representation learning by masked prediction of hidden units," *TASLP*, vol. 29, pp. 3451–3460, 2021.
- [29] S. Chen, C. Wang, Z. Chen, Y. Wu, S. Liu, Z. Chen, J. Li, N. Kanda, T. Yoshioka, X. Xiao *et al.*, "Wavlm: Large-scale self-supervised pre-training for full stack speech processing," *J-STSP*, vol. 16, no. 6, pp. 1505–1518, 2022.
- [30] K. Choi, A. Pasad, T. Nakamura, S. Fukayama, K. Livescu, and S. Watanabe, "Self-supervised speech representations are more phonetic than semantic," in *Proc. Interspeech*, 2024.
- [31] W.-C. Huang, Y.-C. Wu, and T. Hayashi, "Any-to-one sequence-to-sequence voice conversion using self-supervised discrete speech representations," in *Proc. ICASSP*, 2021.
- [32] F. Kreuk, A. Polyak, J. Copet, E. Kharitonov, T.-A. Nguyen, M. Rivière, W.-N. Hsu, A. Mohamed, E. Dupoux, and Y. Adi, "Textless speech emotion conversion using discrete & decomposed representations," in *Proc. EMNLP*, 2022.
- [33] H.-S. Oh, S.-H. Lee, D.-H. Cho, and S.-W. Lee, "Durflex-vcv: Duration-flexible emotional voice conversion leveraging discrete representations without text alignment," *IEEE Transactions on Affective Computing*, 2025.
- [34] E. Kharitonov, D. Vincent, Z. Borsos, R. Marinier, S. Girgin, O. Pietquin, M. Sharifi, M. Tagliasacchi, and N. Zeghidour, "Speak, read and prompt: High-fidelity text-to-speech with minimal supervision," *Trans. ACL*, vol. 11, pp. 1703–1718, 2023.
- [35] K. Lakhotia, E. Kharitonov, W.-N. Hsu, Y. Adi, A. Polyak, B. Bolte, T.-A. Nguyen, J. Copet, A. Baevski, A. Mohamed *et al.*, "On generative spoken language modeling from raw audio," *Trans. ACL*, vol. 9, pp. 1336–1354, 2021.
- [36] A. Lee, P.-J. Chen, C. Wang, J. Gu, S. Popuri, X. Ma, A. Polyak, Y. Adi, Q. He, Y. Tang, J. Pino, and W.-N. Hsu, "Direct speech-to-speech translation with discrete units," in *Proc. ACL*, 2022.
- [37] Q. Fang, S. Guo, Y. Zhou, Z. Ma, S. Zhang, and Y. Feng, "Llama-omni: Seamless speech interaction with large language models," *arXiv preprint arXiv:2409.06666*, 2024.

- [38] M. Cui, D. Tan, Y. Yang, D. Wang, H. Wang, X. Chen, X. Chen, and X. Liu, "Exploring ssl discrete tokens for multilingual asr," in *Proc. ICASSP 2025*, 2025.
- [39] M. Cui, Y. Yang, J. Deng, J. Kang, S. Hu, T. Wang, Z. Li, S. Zhang, X. Chen, and X. Liu, "Exploring ssl discrete speech features for zipformer-based contextual asr," in *Proc. Interspeech 2025*, 2025.
- [40] K. Onda, S. Fukayama, D. Saito, and N. Minematsu, "Advanced modeling of interlanguage speech intelligibility benefit with 11-12 multi-task learning using differentiable k-means for accent-robust discrete token-based asr," in *Proc. ICASSP 2026*, 2026.
- [41] E. Hoogeboom, D. Nielsen, P. Jaii, P. Forré, and M. Welling, "Argmax flows and multinomial diffusion: Learning categorical distributions," in *Advances in neural information processing systems*, vol. 34, 2021, pp. 12 454–12 465.
- [42] J. Austin, D. D. Johnson, J. Ho, D. Tarlow, and R. van den Berg, "Structured denoising diffusion models in discrete state-spaces," in *Advances in Neural Information Processing Systems*, 2021.
- [43] H. Chang, H. Zhang, L. Jiang, C. Liu, and W. T. Freeman, "Maskgit: Masked generative image transformer," in *Proceedings of the IEEE/CVF conference on computer vision and pattern recognition*, 2022, pp. 11 315–11 325.
- [44] Y. Wang, H. Zhan, L. Liu, R. Zeng, H. Guo, J. Zheng, Q. Zhang, X. Zhang, S. Zhang, and Z. Wu, "MaskGCT: Zero-shot text-to-speech with masked generative codec transformer," in *The Thirteenth International Conference on Learning Representations*, 2025. [Online]. Available: <https://openreview.net/forum?id=ExuBFYtCQU>
- [45] Y. Wang, J. Zheng, J. Zhang, X. Zhang, H. Liao, and Z. Wu, "Metis: A foundation speech generation model with masked generative pre-training," in *The Thirty-ninth Annual Conference on Neural Information Processing Systems*, 2025. [Online]. Available: <https://openreview.net/forum?id=RTjr4DnS79>
- [46] R. Yu, Q. Li, and X. Wang, "Discrete diffusion in large language and multimodal models: A survey," 2025. [Online]. Available: <https://arxiv.org/abs/2506.13759>
- [47] A. Lou, C. Meng, and S. Ermon, "Discrete diffusion modeling by estimating the ratios of the data distribution," in *ICML 2024*, 2024.
- [48] G. Wang, Y. Schiff, S. S. Sahoo, and V. Kuleshov, "Remasking discrete diffusion models with inference-time scaling," in *The Thirty-ninth Annual Conference on Neural Information Processing Systems*, 2025. [Online]. Available: <https://openreview.net/forum?id=IJryQA0y0p>
- [49] H. Ben-Hamu, I. Gat, D. Severo, N. Nolte, and B. Karrer, "Accelerated sampling from masked diffusion models via entropy bounded unmasking," in *The Thirty-ninth Annual Conference on Neural Information Processing Systems*, 2025. [Online]. Available: <https://openreview.net/forum?id=WbCbHT1NKO>
- [50] Z. Huang, Y. Wang, Z. Chen, and G.-J. Qi, "Don't settle too early: Self-reflective remasking for diffusion language models," *arXiv preprint arXiv:2509.23653*, 2025.
- [51] S. Zhang, F. Z. Peng, Y. Zhang, J. Pan, and G. G. Chrysos, "Corrective diffusion language models," 2026. [Online]. Available: <https://arxiv.org/abs/2512.15596>
- [52] Y. Song, Z. Zhang, C. Luo, P. Gao, F. Xia, H. Luo, Z. Li, Y. Yang, H. Yu, X. Qu *et al.*, "Seed diffusion: A large-scale diffusion language model with high-speed inference," *arXiv preprint arXiv:2508.02193*, 2025.
- [53] T. Bie, M. Cao, X. Cao, B. Chen, F. Chen, K. Chen, L. Du, D. Feng, H. Feng, M. Gong *et al.*, "Llada2. 1: Speeding up text diffusion via token editing," *arXiv preprint arXiv:2602.08676*, 2026.
- [54] Y. A. Li, C. Han, X. Jiang, and N. Mesgarani, "Hiftnet: A fast high-quality neural vocoder with harmonic-plus-noise filter and inverse short time fourier transform," *arXiv preprint arXiv:2309.09493*, 2023.
- [55] J. Ho and T. Salimans, "Classifier-free diffusion guidance," in *NeurIPS 2021 Workshop on Deep Generative Models and Downstream Applications*, 2021.
- [56] W. Peebles and S. Xie, "Scalable diffusion models with transformers," in *Proc. ICCV*, 2023, pp. 4195–4205.
- [57] Y. Lipman, R. T. Q. Chen, H. Ben-Hamu, M. Nickel, and M. Le, "Flow matching for generative modeling," in *ICLR*, 2023.
- [58] J. Su, M. Ahmed, Y. Lu, S. Pan, W. Bo, and Y. Liu, "Roformer: Enhanced transformer with rotary position embedding," *Neurocomputing*, vol. 568, p. 127063, 2024.
- [59] H. He, Z. Shang, C. Wang, X. Li, Y. Gu, H. Hua, L. Liu, C. Yang, J. Li, P. Shi *et al.*, "Emilia: An extensive, multilingual, and diverse speech dataset for large-scale speech generation," in *2024 IEEE Spoken Language Technology Workshop (SLT)*. IEEE, 2024, pp. 885–890.
- [60] Y. Koizumi, H. Zen, S. Karita, Y. Ding, K. Yatabe, N. Morioka, M. Bacchiani, Y. Zhang, W. Han, and A. Bapna, "LibriTTS-R: A Restored Multi-Speaker Text-to-Speech Corpus," in *Proc. Interspeech*, 2023.
- [61] G. Zhao, S. Sonsaat, A. Silpachai, I. Lucic, E. Chukharev-Hudilainen, J. Levis, and R. Gutierrez-Osuna, "L2-ARCTIC: A Non-native English Speech Corpus," in *Proc. Interspeech*, 2018.
- [62] J. Kominek and A. W. Black, "The cmu arctic speech databases," in *Fifth ISCA workshop on speech synthesis*, 2004.
- [63] S. Mehta, R. Tu, J. Beskow, É. Székely, and G. E. Henter, "Matcha-tts: A fast tts architecture with conditional flow matching," in *Proc. ICASSP*, 2024, pp. 11 341–11 345.
- [64] M. Lewis, "Bart: Denoising sequence-to-sequence pre-training for natural language generation, translation, and comprehension," *arXiv preprint arXiv:1910.13461*, 2019.
- [65] A. Radford, J. W. Kim, T. Xu, G. Brockman, C. McLeavey, and I. Sutskever, "Robust speech recognition via large-scale weak supervision," in *ICML*, 2023, pp. 28 492–28 518.
- [66] Z. Du, Y. Wang, Q. Chen, X. Shi, X. Lv, T. Zhao, Z. Gao, Y. Yang, C. Gao, H. Wang *et al.*, "Cosyvoice 2: Scalable streaming speech synthesis with large language models," *arXiv preprint arXiv:2412.10117*, 2024.
- [67] A. M. V. Ravillion, "A comparison of best-worst scaling and rating scale for timbre characterisation," 2020.
- [68] C. Churchwell, M. Morrison, and B. Pardo, "High-fidelity neural phonetic posteriorgrams," in *ICASSP 2024 Workshop on Explainable Machine Learning for Speech and Audio*, 2024.
- [69] M. McAuliffe, M. Socolof, S. Mihuc, M. Wagner, and M. Sonderegger, "Montreal forced aligner: Trainable text-speech alignment using kaldii," in *Proc. Interspeech*, 2017, pp. 498–502.
- [70] A. van den Oord, O. Vinyals, and K. Kavukcuoglu, "Neural discrete representation learning," in *Proceedings of the 31st International Conference on Neural Information Processing Systems*, 2017, p. 6309–6318.